Atmospheric Environment 253 (2021) 118358

Contents lists available at ScienceDirect

Atmospheric Environment

journal homepage: http://www.elsevier.com/locate/atmosenv

Can light absorption of black carbon still be enhanced by mixing with absorbing materials?

Xue Feng [a,b], Jiandong Wang [a,b,*], Shiwen Teng [a,b], Xiaofeng Xu [a,b], Bin Zhu [a,b], Jiaping Wang [f], Xijuan Zhu [c], Maxim A. Yurkin [d,e], Chao Liu [a,b]

[a] Collaborative Innovation Center on Forecast and Evaluation of Meteorological Disasters, Nanjing University of Information Science and Technology, Nanjing, 210044, China
[b] Key Laboratory for Aerosol-Cloud-Precipitation of China Meteorological Administration, School of Atmospheric Physics, Nanjing University of Information Science and Technology, Nanjing, 210044, China
[c] Science and Technology on Optical Radiation Laboratory, Beijing, 100854, China
[d] Voevodsky Institute of Chemical Kinetics and Combustion SB RAS, Institutskaya str. 3, 630090, Novosibirsk, Russia
[e] Novosibirsk State University, Pirogova Str. 2, 630090, Novosibirsk, Russia
[f] Joint International Research Laboratory of Atmospheric and Earth System Sciences, School of Atmospheric Sciences, Nanjing University, Nanjing, 210023, China

HIGHLIGHTS

- Partially mixed BC and BrC result in similar optical properties to external mixing, but different from the internal mixing.
- Internal BC-BrC mixing would not enhance absorption at short wavelength due to stronger shielding effect over lensing effect.
- Smaller aerosol AAE values would be obtained if BC and BrC are well internally mixed.
- BC and BrC mixing states would significantly affect their attribution.

GRAPHICAL ABSTRACT

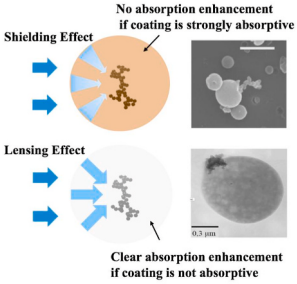

ARTICLE INFO

Keywords:
Black carbon
Brown carbon
Light absorption enhancement
Absorbing aerosols

ABSTRACT

Strongly absorbing black carbon (BC) particles are commonly mixed with other aerosols in the ambient atmospheres, resulting in absorption enhancement known as the lensing effect. If other absorbing aerosols such as mineral dust and brown carbons (BrCs) are mixed with BC particles, resulting absorption properties are still less certain. Such mixtures are common due to large amounts of BrC (and tarballs) co-emitted with BC from biomass burning. Thus, this study focuses on mixtures of two absorbing carbonaceous aerosols with different spectral variations of absorption, and reveals the influences of mixing states on their absorption, especially on their spectral variation and enhancement. Three typical mixing states (internally, partially and externally mixed) and complex nonspherical BC structures (fractal aggregates) are considered accurately in the light scattering simulations. The absorption Angstrom exponent (AAE) of internally mixed particles can increase to over 2 when BrC volume fraction is above 70%, but it is systematically smaller (by up to 0.1) than those of the partially mixed and externally mixed particles. Different from non-absorbing coating acting as a lens, internal mixing of BC and BrC may not enhance BC absorption at shorter wavelengths, while the total absorption may even be reduced due to

* Corresponding author. Collaborative Innovation Center on Forecast and Evaluation of Meteorological Disasters, Nanjing University of Information Science and Technology, Nanjing, 210044, China.
E-mail address: jiandong.wang@nuist.edu.cn (J. Wang).

https://doi.org/10.1016/j.atmosenv.2021.118358
Received 23 November 2020; Received in revised form 26 February 2021; Accepted 17 March 2021
Available online 22 March 2021

the "protection" of BC by the BrC coating, referred to as a "shielding effect". Specifically, absorption enhancement in the case of internal mixing is sensitive to coating absorptivity (influenced by both its refractive index and volume fraction), and becomes close to or even smaller than 1 as the coating becomes more absorbing. Furthermore, the mixing states of two absorbing aerosols would surely affect absorption attribution as well as downstream estimations of BC heating effects. Thus, it should be carefully considered in future studies.

1. Introduction

Carbonaceous aerosols, usually generated from biomass combustion and composed of black carbon (BC) and organic carbon (OC) (China et al., 2013; Ito et al., 2005). BC is one of the strongest light absorbing aerosols, and some organic carbon components moderately absorb light from the ultraviolet to visible wavelengths as well, which is known as brown carbon (BrC) (Kirchstetter et al., 2004; Cappa et al., 2012). These light absorbing carbon aerosols play a significant warming role on the climate, which are still one of the most uncertain components on aerosol effects and climate change studies (Andreae et al., 2006; Bond et al., 2006; Bergstrom et al., 2007; Lack et al., 2012).

Estimations of the radiative properties and effects of BC-containing aerosols are still of large uncertainties. One of the main reasons is relatively poor quantitative understanding on the optical properties of those BC aerosols in the ambient atmosphere. The mass absorption cross section (MAC) is a fundamental variable to quantify aerosol absorption capability, especially those of BC (Jacobson et al., 2001), whereas MAC of BC still has great uncertainties from both observational and numerical studies. To be specific, BC from different regions or emission sources show MACs ranging from 5.2 up to 19.3 m^2/g (Martins et al., 1998), and a similar range (3.4–16.8 m^2/g) is reported by Ram et al. (2009). By reviewing previous studies, a fresh BC MAC at an incident wavelength of 550 nm is suggested to be 7.5 ± 1.2 m^2/g (Bond and Bergstrom, 2006), and it is widely used in global aerosol modelling studies. However, compared to absorption of fresh BC, the absorption of aged BC (those normally mixed with other aerosols) may increase, and the absorption enhancement, specified by the ratio of aged/mixed BC absorption to that of fresh BC, is reported to be ranging from negligible (~1) to significant (~3.5) (Schnaiter et al., 2005; Cappa et al., 2012; Cheng et al., 2014a,b; J. Wang et al., 2018a). Another important variable represents spectral variations of aerosols is referred to as the absorption Angstrom exponent (AAE). BC AAE is also not a fixed value, because it can be affected by multiple effects such as particle size, mixing state and morphology (Utry et al., 2014; Liu et al., 2015; Wu et al., 2018). Thus, the warming effects caused by BC-containing particles is complex which depends not only on BC microphysical characteristics but also particles mixing states (Cappa et al., 2012; Adachi et al., 2010; Liu et al., 2015; Wu et al., 2018).

BC is often mixed with organic material (China et al., 2013; Ito et al., 2005). Utry et al. (2014) found that environmental AAE are greatly affected by ratio of OC to elemental carbon, suggesting that both organic and elemental carbons play important roles in aerosol light absorption (BrC is known as part of organic carbon). Moreover, there is a large amount of BrC co-emitted from biomass burning (Pósfai et al., 2003; Yuan et al., 2020; Chen et al., 2021). Yuan et al. (2020) found that approximately 28% of thousands of individual particles collected on the northern slope of the Himalayas are tarballs, and the contribution of tarball-containing particles may increase to over 50% on polluted days. An even higher tarball fraction of 80% is observed in the vicinity of biomass burning sources (Pósfai et al., 2003). Moreover, field observations show that BrC has higher absorption efficiency at wavelengths between 300 and 400 nm, and may contribute over 30% to aerosol total light absorption at the spectrum (Hoffer et al., 2006; Yang et al., 2008; Cheng et al., 2015). Even in the entire solar spectrum, the relatively contribution of BrC to light absorption can still reach 6.4–8.6% (Hoffer et al., 2006; Srinivas et al., 2013). Thus, although BC plays a leading role in aerosols absorption in the atmosphere, the contribution of BrC cannot be ignored especially from biomass combustion.

The optical properties of BC mixed with weakly- or non-absorbing aerosols have been extensively studied using both numerical simulations and observations (Lack and Cappa, 2010; Schnaiter et al., 2005; Bond et al., 2006). However, with significant amount of BrC in the atmosphere, especially from biomass burning, the unnegligible absorption of BrC at shorter wavelengths and its spectral variations make aerosol absorption properties more complex, not even mentioning mixtures of different absorbing materials. This raises the questions: would the absorption of BC and BrC mixtures be also enhanced? How would the absorption of two absorbing components be influenced by mixing? This study tries to answer those questions and to reveal the effect of mixing BC with other absorbing materials. The paper is organized as the following. Section 2 introduces the numerical models used for mixed aerosols with complex nonspherical BC geometries and mixing states. The influences of mixing states on the spectral absorption and absorption enhancement are discussed in Section 3, and Section 4 shows an example to demonstrate the further influences of such mixing on the absorption material attribution. Section 5 concludes the paper.

2. Methods

Realistic representations of aerosol microphysical and mixing properties are essential for their optical and radiative property studies. In contrast to spheres, BC particles show highly complicated aggregated morphology in the atmosphere (Chakrabarty et al., 2006; Wang et al., 2017). A fractal aggregate model, parameterized as $N = k_f\left(\frac{R}{a}\right)^{D_f}$, is widely used. Here, N is monomer number, a is monomer radius, k_f is the fractal prefactor, D_f is the fractal dimension, and R is the radius of gyration. By changing k_f and D_f, the morphology of BC aggregate can be numerically generated. More details can be found in Sorensen (2001).

After emitted, fresh BC particles undergo the so-called 'aging' process during which BC are mixed with different materials in the atmosphere, and often become coated by or attached with other aerosol components (e.g., by sulphate or sea salt) (Wang et al., 2018b; Liu et al., 2016; Moteki et al., 2007; Cheng et al., 2014a,b; Huang et al., 2014). Observations indicate that resulting aerosols can be mixed to different degrees (China et al., 2013). To better investigate the optical properties of aged BC aerosols in details, we consider three mixing states, i.e., internally, partially and externally mixed ones. Different from most of previous studies that have the internally and externally mixed cases, this study considers a partially mixed case as well, which can be understood as a state between the internal and external ones. For better explanation, three examples of microscopic images of observed BC particles and the corresponding sketches are shown in Fig. 1. We use fractal aggregates to represent BC particles, and spheres to represent the BrC component. Here, the BC aggregates have 50 monomers and a D_f of 1.8. The internally mixed model (IM, Fig. 1a) implies that the BC core is well coated at the center of the BrC sphere, and the partially mixed case (PM, Fig. 1b) means that the two components contact only at their boundaries. The externally mixed model (EM, Fig. 1c) represents the case when the BC aggregate and the spherical component exist separately in the same atmosphere (and are sufficiently isolated from each other). Here, we define the BC volume fraction F_{BC} as the ratio of the BC component to the total volume of the mixture. Small F_{BC} indicates BC particles that are heavily coated by BrC, while large F_{BC} indicates BC-dominant mixtures. Specifically, we perform simulations with F_{BC} between 0.01 and 0.99.

Given the three mixing models, we use the discrete dipole

approximation (DDA) (Yurkin et al., 2007) to calculate the orientation-averaged optical properties. In the framework of the DDA, any particle is discretized into small sub-volumes (namely dipoles); the set of such dipoles can approximate any three-dimensional particle shape. It should be noticed that both internally mixed and partially mixed particles in Fig. 1(a) and (b) are treated as single particles for optical simulations, so their electromagnetic interactions are rigorously accounted for. However, the externally mixed particles consider BC and BrC particles separately, and the resulting optical properties are combined to give those of the mixture. To better represent those particles with complex structures, a relatively high resolution is needed – we used 50, dipoles per wavelength which corresponds to at least ~170 dipoles per diameter of a BC constituent sphere. The state-of-art DDA implementation (Yurkin and Hoekstra, 2011) is used in this study, specifically ADDA v.1.3, which has been previously shown to be sufficiently accurate and efficient for BC related simulations (Liu et al., 2018).

AAE is normally used to represent spectral variations of aerosol absorption properties, by the approximation of $A_\lambda = A_o\lambda^{-AAE}$, so it is defined as:

$$AAE = -\frac{\ln(A_1/A_2)}{\ln(\lambda_1/\lambda_2)}$$

Here, A_1 and A_2 are the absorption cross sections at the wavelengths of λ_1 and λ_2, respectively. The AAE in this study will be calculated based on the absorption at incident wavelengths of 370 nm and 880 nm from our numerical simulations or the Model AE-33 aethalometer (Magee Scientific, USA).

Another important quantity is the absorption enhancement (E_{BC}), i.e., the ratio of the absorption cross section of coated/mixed BC to the uncoated/unmixed one. With second absorbing component, its contribution should be removed for E_{BC} calculation. Thus, E_{BC} is rewritten as:

$$E_{BC} = \frac{A_{mixture} - A_{coating}}{A_{BC}}$$

where $A_{mixture}$, $A_{coating}$, and A_{BC} are the absorption cross sections of mixture (BC + BrC as a mixture, i.e., internally, partially or externally mixed) and independently coating/BrC and BC components, respectively. Again, the E_{BC} indicates the influence of mixing process on BC absorption, i.e. it always equals one for external mixtures.

This study fixes the k_f and D_f of BC aggregates at their commonly used values of 1.2 and 1.8, respectively (Sorensen et al., 2001; Bond et al., 2006). The diameter of monomers is assumed to be 30 nm (Sorensen et al., 2001). The details on the fractal aggregates model as well as their generation in this study can be found in Liu et al. (2018). We ignore the minor irregular structures of aggregates, because their effects are normalized by considering MAC (Teng et al., 2020). Furthermore, BC often satisfies a lognormal size distribution in terms of the geometric mean radii (R_g) of corresponding equivalent volume spheres (Liu et al., 2006), and all our results discussed are bulk optical properties averaged over given size distributions (Li et al., 2016). For the latter we consider the R_g range between 0.06 and 0.15 μm and a standard deviation of 1.5. Note that when F_{BC} is fixed, the size of both BC and BrC components scale with R_g. In particular, the radius of the BrC component is significantly smaller or larger than R_g for F_{BC} close to 1 or 0, respectively. For a fair comparison, we fixed all other variables making the mixing state as the only control variable.

The wavelength-dependent refractive indices (RIs) are another fundamental parameter influencing the aerosol optical properties (He et al., 2015). BrC appears to be yellow or brown because its absorption highly depends on the wavelength – it absorbs solar radiation more efficiently at shorter than at longer wavelengths. The RIs of BC are from D'Almeida et al. (1991), while there are still significant uncertainties on BrC RIs, i.e. quite different results are observed or retrieved (Alexander et al., 2008; Chakrabarty et al., 2010; Hoffer et al., 2016). To account for this uncertainty, we performed simulations for two different datasets of BrC RIs: Hoffer et al. (2016) and Alexander et al. (2008), the corresponding results are further denoted by "BrC-H" and "BrC-A", respectively. We consider optical properties at six wavelengths, and the corresponding BrC RIs based on Hoffer et al. (2016) are obtained by interpolation. Fig. 2 illustrates the RIs of BC and BrC. The most significant differences of the imaginary parts of their RIs are the spectral variations. BC shows almost constant value over the visible and near infrared region, while the corresponding BrC value decreases as wavelength increases, which is the reason for its brown color.

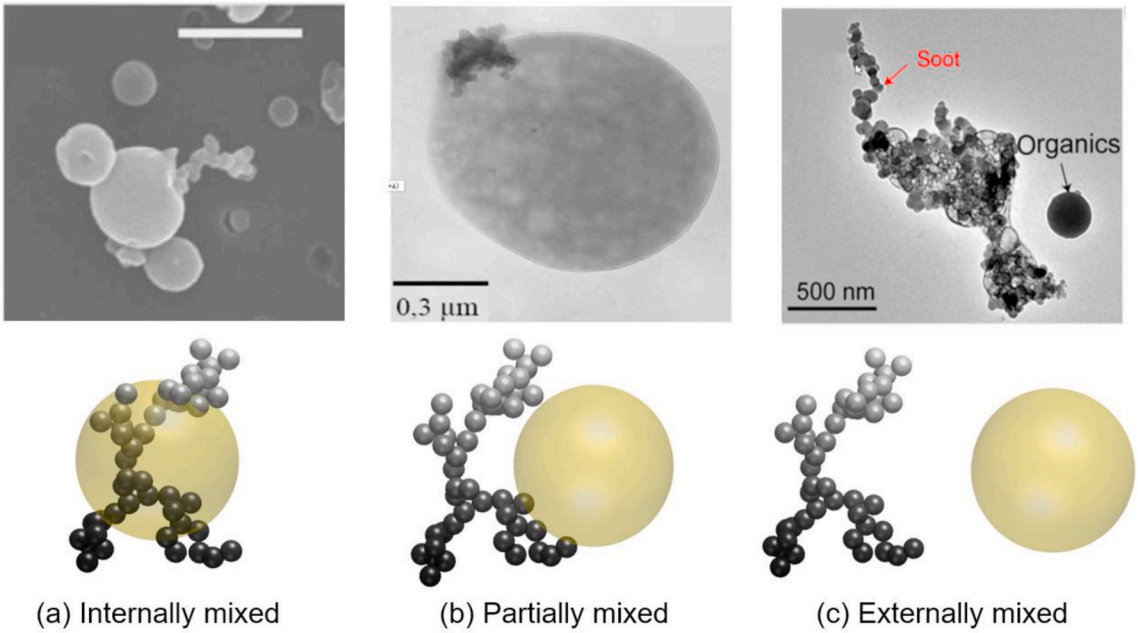

Fig. 1. Microscopic images (Wang et al., 2017; China et al., 2013; Kahnert et al., 2012) and model of BC-containing particles. The BC aggregates (small black spheres) are internally mixed (a), partially mixed (b) and externally mixed (c) with the spherical organic component (yellow spheres). The BC aggregate consists of 50 monomers and $F_{BC} = 0.5$. (For interpretation of the references to color in this figure legend, the reader is referred to the Web version of this article.)

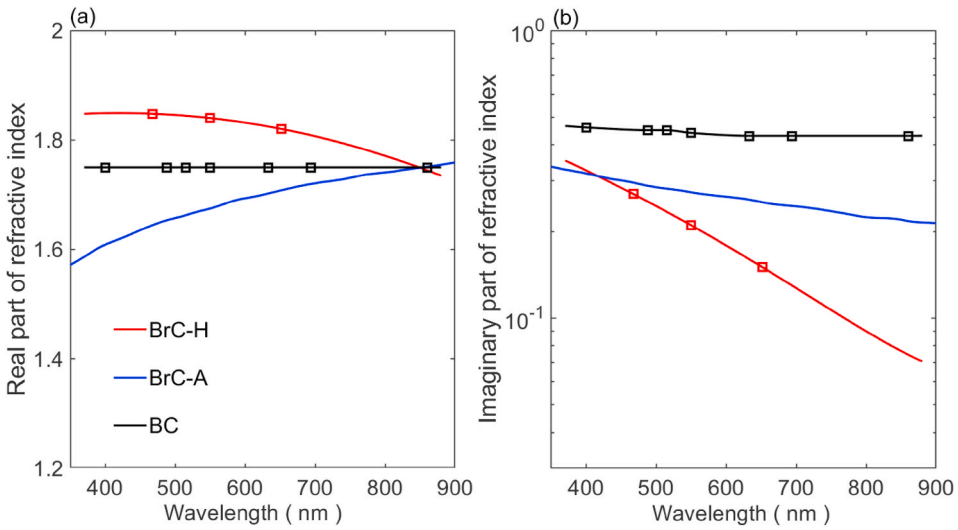

Fig. 2. The real (a) and imaginary part (b) of refractive indices of black carbon (D'Almeida et al., 1991) and brown carbon aerosols (Hoffer et al., 2016; Alexander et al., 2008 – red and blue lines, respectively). (For interpretation of the references to color in this figure legend, the reader is referred to the Web version of this article.)

3. Light absorption properties

Fig. 3 shows mixture AAE as a function of F_{BC} and R_g, and the top and bottom panels are for AAEs based on different RIs of BrC: AAE-H, and AAE-A, respectively. The left column shows the results of externally mixed particles as references. In particular, AAE is less dependent on R_g when BrC coating is less dominant, i.e., F_{BC} larger than 0.5 – this is similar to AAE of pure BC. For mixtures with F_{BC} less than 0.5, AAE-H

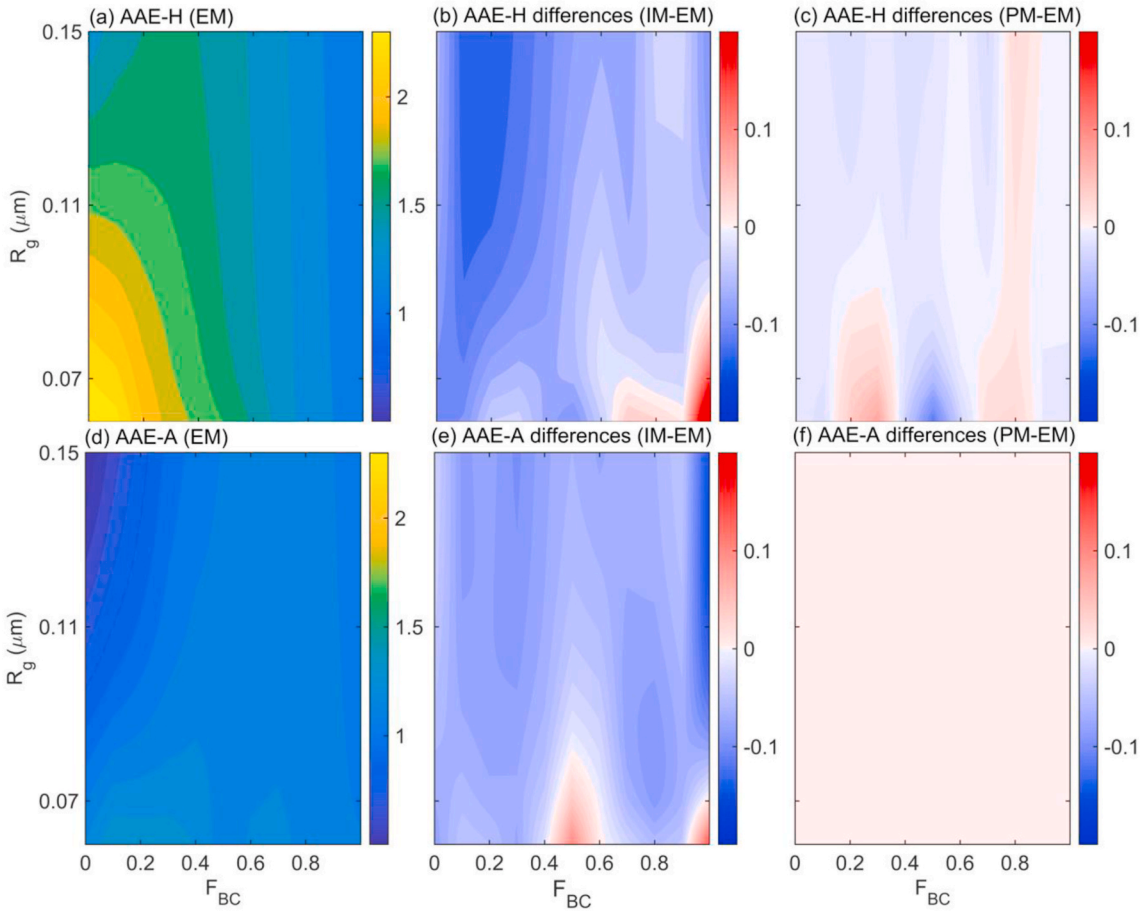

Fig. 3. AAE of mixtures with different BC equivalent radius (R_g) and volume fraction (F_{BC}). (a) and (d) are the AAE for externally mixed particles. (b) and (e) show the differences between the internally and externally mixed, and (c) and (f) show the differences between the partially and externally mixed cases. The top row is based on BrC RI from Hoffer et al. (2016) and the second row – from Alexander et al. (2008).

becomes more sensitive to R_g, increasing from ~1.4 to 2.5 with F_{BC} and R_g decreasing. The maximum value is determined by strong wavelength dependence of imaginary part of BrC RI from Hoffer et al. (2016), while the remaining variation of AAE with R_g for very small F_{BC} is due to the fact, that the size of the BrC component is then comparable to the wavelength, under which condition size largely affects AAE. The AAE-A, mostly around 1, is markedly different from AAE-H (Fig. 3d), due to much smaller spectral dependence of the imaginary part of corresponding BrC RI. The differences on the AAE between internally and externally mixed particles, i.e., IM–EM, are shown in the middle panels. Generally, the internal mixing results in smaller AAE, especially under small F_{BC} conditions. This is because internally mixed structure enhances absorption at longer wavelengths, but not so much at shorter ones. Meanwhile, the differences between the externally mixed and partially mixed particles, given in Figs. 3c and 3f, are much smaller with absolute values within 0.05. This means that only after BC and BrC are well internally mixed, their absorption can change significantly, while partially mixed particles result in little differences on particle absorption from externally mixed ones.

To better understand the behaviour of AAE, we compare the corresponding E_{BC} throughout the visible and near infrared wavelengths. Fig. 4 shows E_{BC} for the internally mixed and partially mixed particles, using the externally mixed model as a reference, and BrC-H is considered here as an example. E_{BC} of the partially mixed particles is mostly around unit (right panel), and non-trivial results are obtained only if BC and BrC-H are well internally mixed (left panel). In the latter case E_{BC} is very sensitive to the incident wavelength. As the wavelength increases, BrC-H becomes less absorptive leading to the increase of E_{BC} (due to the lensing effect). By contrast, E_{BC} is less than 1 for wavelengths less than ~600 nm, which means that the absorption of the internally mixed particles is less than the sum of its two components (when they are externally mixed). This corresponds to the relatively strong absorption of BrC-H at shorter wavelengths. Not surprisingly, this E_{BC} being less than 1 (i.e. absorption reduction instead of enhancement) is different from previous results (Schnaiter et al., 2005; Bond et al., 2006), which are mostly based on non-absorbing second components.

The spectral differences on E_{BC} with BrC-A coating would surely differ due to the different RI imaginary part variations, so, to further account for uncertainties of the RI of BrC and other potential coating materials, we fix the geometry of the internally mixed particle and independently vary real and imaginary parts of the coating RI. Fig. 5 illustrates the E_{BC} at different RIs. Specifically, we set $F_{BC} = 0.05$, i.e. a large fraction of the coating, the incident wavelength to 520 nm, and $R_g = 0.13$ μm (belonging to the accumulation mode). The yellow diamonds indicate the RIs of some typical aerosols (Moffet et al., 2009; Diner et al., 1994; Hess et al., 1998) and the grey diamonds illustrate BrC RIs from different references (Alexander et al., 2008; Chakrabarty et al., 2010; Hoffer et al., 2016) and wavelengths. Clearly, E_{BC} decreases with the increase of the RI imaginary part or the decrease of the real part. This can be explained by the sketches shown in the left panel of Fig. 5. With the increase of the coating absorption (the upper sketch), i.e., larger imaginary part of the coating RI, the scattered light 'inside' the particle (that actually acts on BC) becomes weaker, resulting in the reduction of absorption due to BC, and we define this influence as a "shielding effect". The bottom left panel is an illustration for the so-called "lensing effect", where the coating acts as a lens that focuses energy on the BC "core" enhancing its absorption (Bond et al., 2006). Although both cases result in total absorption larger than that of bare BC particles, the former is contributed by the intrinsic absorption of BrC materials, while the latter is caused by the lensing effect. Note that the threshold for absorption enhancement and reduction of the RI may change under different F_{BC} conditions. Again, the results of partially mixed particles are similar to those of externally mixed (Fig. 4b), so the corresponding results for E_{BC} are not shown.

4. Consequences for light absorption attribution

We discuss the importance of mixing states of two absorbing components by considering their attribution. Since BC tends to have AAE close to 1 and BrC is supposed to have larger AAE, the AAE can be used to attribute absorption from BC and BrC or their volume fractions. However, different assumptions on their mixing states would clearly lead to differences on estimation of their fractions from measured AAE. To be more specific, we determine the BC and BrC fractions by matching observed AAE values with simulated ones of the mixture. This attribution may be not as rigorous as the traditional one that assumes a BC AAE of 1 and none BrC absorption at longer wavelengths (Lack and Langridge, 2013), but it is reasonably enough to illustrate the effect of different BC and BrC mixing states. We consider aerosol absorption obtained from a Model AE-33 Aethalometer (Drinovec et al., 2015). The observation is taken at the suburb of Nanjing, China. Results over four days between August 12–16, 2018 are discussed. The details on the measurements can be found in Tan et al. (2020).

Fig. 6 is an example of aerosol spectral absorption measured by the AE-33 device at August 14, 2018. The sample has aerosol absorption coefficient of 65 Mm^{-1} at 370 nm, and AAE of 1.57. For the traditional attribution, assuming that absorption at 880 nm is solely due to BC and that BC has an AAE of 1, we obtain the black region as the BC-contributed absorption. The remaining region, then, corresponds to BrC; in particular, the latter contributes 38% of the total absorption at the 370 nm. Such an attribution is the traditional one that cannot consider BC mixing states. However, the mixing state would directly influence aerosol mass absorption coefficients, and a fixed BC AAE of 1 for the attribution would also introduce certain errors. Thus, we try to use the AAE of the mixture as the indicator for the absorption and BC/BrC attribution. For the simplest illustration, we use the results from

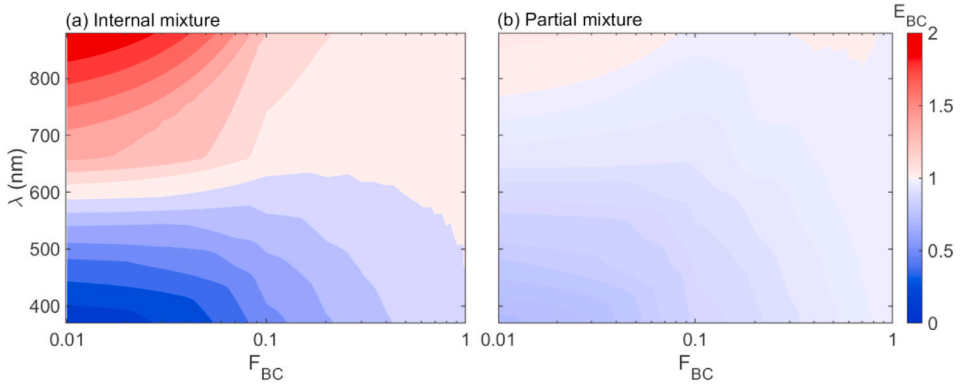

Fig. 4. E_{BC} due to mixing with BrC-H as a function of F_{BC} throughout the visible and near-infrared wavelengths for (a) internally mixed and (b) partially mixed models. The logarithmic scale is used for the horizontal axis.

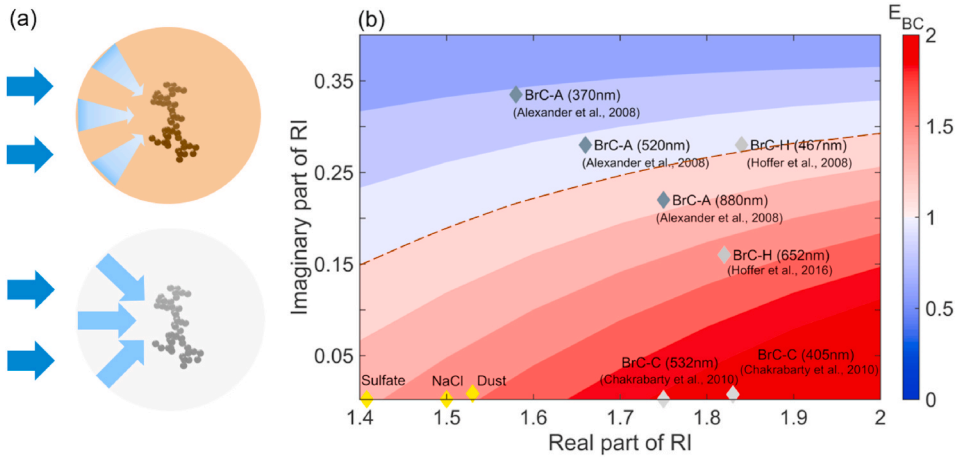

Fig. 5. E_{BC} of internally mixed particle as a function of the coating RIs. All other problem parameters are fixed (see the text). The yellow and grey diamond represent the RI of some typical aerosol materials, other than BC. For BrC, the RI values at several different wavelengths are shown. (For interpretation of the references to color in this figure legend, the reader is referred to the Web version of this article.)

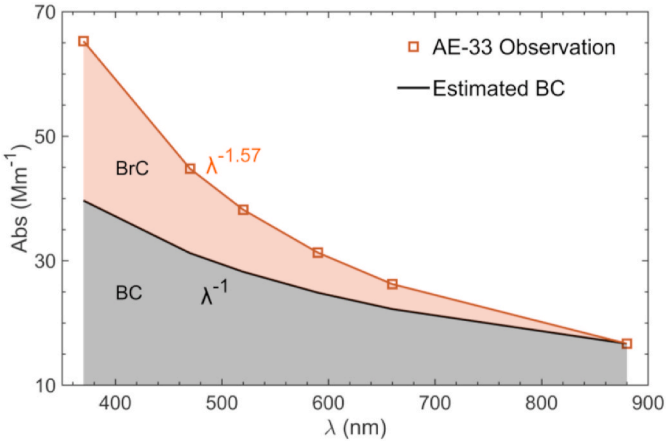

Fig. 6. An example of the absorption attribution from the traditional method. See the text for details.

Fig. 3 (top row) and assume a fixed $R_g = 0.13$ μm (for BC component) and internal mixing between BC and BrC-H, so AAE = 1.57 corresponds to $F_{BC} = 32\%$. In other words, the internal mixture with 32% BC and 68% BrC-H corresponds to a simulated AAE of 1.57. Importantly, here and further we consider BrC-H (having the largest AAE) for quantitative estimation. If, however, the components are assumed to be partially mixed or externally mixed, the retrieved F_{BC} would be 45%, which is over 10% larger than the previous value based on internally mixed particles. This simple estimation is sufficient to demonstrate the importance of mixing states, but a more rigorous attribution should be performed to quantitatively study this effect.

Fig. 7 illustrates aerosol AAE and our estimation of BC volume fractions. Fig. 7a shows the AAE temporal variation over the four days, and hourly averaged results are shown. AAE values vary mostly between 1 and 1.8, and most low values are noticed around noon of the local time. Larger AAE values can be explained by larger BrC fraction in the atmosphere. As mentioned above, F_{BC} is directly estimated from these AAE values. When the AAE is small (~1), the absorbing aerosols are expected to be BC dominant, i.e. F_{BC} to ~1. With the increase of mixture AAE, F_{BC} decreases. We are mostly interested in F_{BC} differences due to

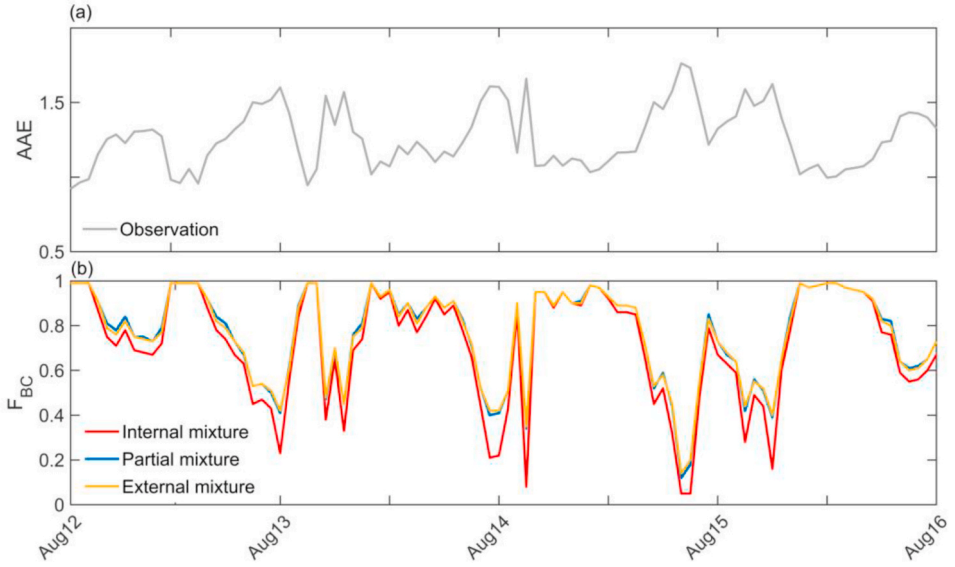

Fig. 7. (a) AAE given by AE-33-based spectral absorption and (b) the corresponding BC and BrC-H attribution (i.e., F_{BC}) based on the measured AAE values during a four-day period in Nanjing, China.

different mixing states. As expected, the differences between the externally mixed and partially mixed cases are negligible. By contrast, the internally mixed results for F_{BC} are significantly smaller than those based on external mixture (by as large as 20% for BrC abundant cases), because the internal mixing reduces the AAE. Note, however, that this effect is partly due to the assumed RI of BrC-H – it may be smaller for other sets of RI or other absorbing materials.

5. Conclusion

This study investigates the bulk absorption of BC aerosols influenced by mixing with absorbing materials, particularly the absorbing carbonaceous aerosol BrC. Three mixing states including internal, partial and external mixing are considered for comparison, and the effects of such mixing and particle nonsphericity are fully considered by applying the discrete dipole approximation for light scattering simulations. Our results indicate that there is little difference on absorption between the optical properties of partially mixed and externally mixed particles if all other variables are fixed. However, the AAE of internally mixed particles is significantly smaller than that of externally mixed ones, especially for those with large BrC coating volume fraction, because the absorption enhancements due to internal mixing varies with the incident wavelengths. Specifically, the internal mixing of BC and BrC may still enhance absorption at longer wavelengths, while its influence on the absorption at shorter wavelengths is less significant. For internally mixed particles, E_{BC} is very sensitive to coating absorption properties, and drops to less than 1 at shorter wavelengths (where BrC is strongly absorbing). For the internally mixed case, the coating properties (the RI and volume fraction) affect the light intensity reaching the BC core. Different from non-absorbing coating that causes significant BC absorption enhancement due to the lensing effect, strong absorption by the coating attenuates light reaching the BC core, resulting in no enhancement or even reduction of BC absorption, which we refer to as a shielding effect.

As a key aerosol microphysical property, the mixing state of BC and BrC particles influences not only the retrieval of their properties but also their radiative forcing, because the absorption properties are quite sensitive to the mixing states. Our findings will be useful for better understanding of the absorption properties of atmospheric aerosols as well as of their radiative effects, so we suggest the mixing states to be better detected in laboratory or in-situ observations and to be better parameterized in future model development.

CRediT authorship contribution statement

Xue Feng: Methodology, Software, Data curation, Writing – original draft, Writing – review & editing. **Jiandong Wang:** Conceptualization, Writing – original draft, Writing – review & editing, Supervision. **Shiwen Teng:** Software, Writing – review & editing. **Xiaofeng Xu:** Data curation, Writing – review & editing. **Bin Zhu:** Data curation, Writing – review & editing. **Jiaping Wang:** Data curation, Writing - review & editing. **Xijuan Zhu:** Methodology, Writing – review & editing. **Maxim A. Yurkin:** Methodology, Writing – review & editing. **Chao Liu:** Conceptualization, designed the research, Conceptualization, Writing – original draft, Writing – review & editing, Supervision.

Declaration of competing interest

The authors declare that they have no known competing financial interests or personal relationships that could have appeared to influence the work reported in this paper.

Acknowledgements

The results are available at https://github.com/ShiwenTeng/BlackCarbon_Absorption. This research was funded by the National Natural Science Foundation of China (42075098), the Natural Science Foundation of Jiangsu Province (BK20190093), and "Qinglan Project" of Jiangsu Province. The development of the ADDA code is supported by the Russian Science Foundation (18-12-00052).

References

Adachi, K., Chung, S.H., Buseck, P.R., 2010. Shapes of soot aerosol particles and implications for their effects on climate. J. Geophys. Res. Atmos. 115, D15206.
Alexander, D.T.L., Crozier, P.A., Anderson, J.R., 2008. Brown carbon spheres in Ease Asian outflow and their optical properties. Science 321, 833–836.
Andreae, M.O., Gelencser, A., 2006. Black carbon or brown carbon? The nature of light-absorbing carbonaceous aerosols. Atmos. Chem. Phys. 6, 3131–3148.
Bergstrom, R.W., Pilewskie, P., Russell, P.B., Redemann, J., 2007. Spectral absorption properties of atmospheric aerosols. Atmos. Chem. Phys. 7, 5937–5943.
Bond, T.C., Bergstrom, 2006. Light absorption by carbonaceous particles: an investigative review. Aerosol Sci. Technol. 40, 27–67.
Cappa, C.D., Onasch, T.B., Massoli, P., Worsnop, D.R., Bates, T.S., Cross, E.S., Davidovits, P., Hakala, J., Hayden, K.L., Jobson, B.T., Kolesar, K.R., Lack, D.A., Lerner, B.M., Li, S., Mellon, D., Nuaaman, I., Olfert, J.S., Petaja, T., Quinn, P.K., Song, C., Subramanian, R., Willianms, E.J., Zaveri, R.A., 2012. Radiative absorption enhancements due to the mixing state of atmospheric black carbon. Science 337, 1078–1081.
Chakrabarty, R.K., Moosmuller, H., Chen, L.W.A., Lewis, K., Arnott, W.P., Mazzoleni, C., Dubey, M.K., Wold, C.E., Hao, W.M., Kreidenweis, S.M., 2010. Brown carbon in tar balls from smoldering biomass combustion. Atmos. Chem. Phys. 10, 6363–6370.
Chakrabarty, R.K., Moosmüller, H., Garro, M.A., Arnott, W.P., Walker, J., Susott, R.A., Babbitt, R.E., Wold, C.E., Lincoln, E.N., Hao, W.M., 2006. Emissions from the laboratory combustion of wildland fuels: particle morphology and size. J. Geophys. Res. Atmos. 111, 135–153.
Chen, P., Kang, S., Abdullaev, S.F., Safarov, M.S., Huang, J., Hu, Z., Tripathee, L., Li, C., 2021. Significant influence of carbonates on determining organic carbon and black carbon: a case study in Tajikistan, Central Asia. Environ. Sci. Technol. https://doi.org/10.1021/acs.est.0c05876.
Cheng, T., Gu, X., Wu, Y., Chen, H., 2014a. Effects of atmospheric water on the optical properties of soot aerosols with different mixing states. J. Quant. Spectrosc. Radiat. Transfer 147, 196–206.
Cheng, T., Wu, Y., Chen, H., 2014b. Effects of morphology on the radiative properties of internally mixed light absorbing carbon aerosols with different aging status. Opt Express 22, 15904–15917.
Cheng, Y., He, K., Du, Z., Engling, G., Liu, J., Ma, Y., Zheng, M., Weber, R., 2015. The characteristics of brown carbon aerosol during winter in Beijing. Atmos. Environ. 127, 355–364.
China, S., Mazzoleni, C., Gorkowski, K., Aiken, A.C., Dubey, M.K., 2013. Morphology and mixing state of individual freshly emitted wildfire carbonaceous particles. Nat. Commun. 4, 2122.
D'Almeida, G.A., Koepke, P., Shettle, E.P., 1991. Atmospheric Aerosols: Global Climatology and Radiative Characteristics. A Deepak Publishing, Hampton, USA.
Diner, D.J., Abdou, W., Ackerman, T., Conel, J., Gordon, H., Kahn, R., Martonchik, J., Paradise, S., Wang, M., West, R., 1994. MISR Level 2 Algorithm Theoretical Basis: Aerosol/surface Product, Part 1 (Aerosolparameters), Rep.JPL-Dl1400, Rev. A, JetPropul. Lab., Pasadena, Calif.
Drinovec, L., Močnik, G., Zotter, P., Prévôt, A., Ruckstuhl, C., Coz, E., Rupakheti, M., Sciare, J., Muller, T., Wiedensohler, A., Hansen, A., 2015. The "dual-spot" Aethalometer: an improved measurement of aerosol black carbon with real-time loading compensation. Atmos. Meas. Tech. 8, 1965–1979.
He, C., Liou, K.N., Takano, Y., Zhang, R., Zamora, M.L., Yang, P., Li, Q., Leung, L.R., 2015. Variation of the radiative properties during black carbon aging: theoretical and experimental intercomparison. Atmos. Chem. Phys. 15, 19835–19872.
Hess, M., Koepke, P., Schult, I., 1998. Optical properties of aerosols and clouds: the software package OPAC. Bull. Am. Meteorol. Soc. 79, 831–844.
Hoffer, A., Gelencser, A., Guyon, P., Kiss, G., Schmid, O., Frank, G., Artaxo, P., Andreae, M.O., 2006. Optical properties of humic-like substances (HULIS) in biomass-burning aerosols. Atmos. Chem. Phys. 6, 3563–3570.
Hoffer, A., Tóth, A., Nyirő-Kósa, I., Pósfai, M., Gelencsér, A., 2016. Light absorption properties of laboratory generated tar ball particles. Atmos. Chem. Phys. 16, 239–246.
Huang, X., Song, Y., Zhao, C., Li, M., Zhu, T., Zhang, Q., Zhang, X., 2014. Pathways of sulfate enhancement by natural and anthropogenic mineral aerosols in China. J. Geophys. Res. Atmos. 119, 14165–14179.
Ito, A., Penner, J.E., 2005. Historical emissions of carbonaceous aerosols from biomass and fossil fuel burning for the period 1870–2000. Global Biogeochem. Cycles 19. https://doi.org/10.1029/2004GB002374.
Jacobson, M.Z., 2001. Strong radiative heating due to the mixing state of black carbon in atmospheric aerosols. Nature 409, 695–697.
Kahnert, M., Nousiainen, T., Lindqvist, H., Ebert, M., 2012. Optical properties of light absorbing carbon aggregates mixed with sulfate: assessment of different model geometries for climate forcing calculations. Opt Express 20, 10042–10058.
Kirchstetter, T.W., Novakov, T., Hobbs, P.V., 2004. Evidence that the spectral dependence of light absorption by aerosols is affected by organic carbon. J. Geophys. Res. Atmos. 109, D21208.
Lack, D.A., Cappa, C.D., 2010. Impact of brown and clear carbon on light absorption enhancement, single scatter albedo and absorption wavelength dependence of black carbon. Atmos. Chem. Phys. 10, 4207–4220.

Lack, D.A., 2012. Carbon to wood smoke particulate matter absorption of solar radiation. Atmos. Chem. Phys. 12, 6067–6072.
Liu, C., Teng, S., Zhu, Y., Yurkin, M., Yung, Y.L., 2018. Performance of discretize dipole approximation for optical property simulations of black carbon aggregates. J. Quant. Spectrosc. Radiat. Transfer 221, 98–109.
Lack, D.A., Langridge, J.M., 2013. On the attribution of black and brown carbon light absorption using the Angstrom exponent. Atmos. Chem. Phys. 13, 10535–10543.
Li, J., Liu, C., Yin, Y., Kumar, K.R., 2016. Numerical investigation on the Ångström Exponent of black carbon aerosols. J. Geophys. Res. Atmos. 121 https://doi.org/10.1002/2015JD024718.
Liu, D., Taylor, J.W., Young, D.E., Flynn, M.J., Coe, H., Allan, J.D., 2015. The effect of complex black carbon microphysics on the determination of the optical properties of brown carbon. Geophys. Res. Lett. 42, 613–619.
Liu, F., Stagg, B.J., Snelling, D.R., Smallwood, G.J., 2006. Effects of Primary Soot Particle Size Distribution on the temperature of soot particles heated by a nanosecond pulsed laser in an atmospheric laminar diffusion flame. Int. J. Heat Mass Tran. 49, 777–788.
Liu, F., You, J., Bescond, A., 2016. On the radiative properties of soot aggregates – Part 2: effects of coating. J. Quant. Spectrosc. Radiat. Transfer 172, 134–145.
Martins, J.V., Artaxo, P., Liousse, C., Reid, J.S., Hobbs, P.V., Kaufman, Y.J., 1998. Effects of black carbon content, particle size, and mixing on light absorption by aerosols from biomass burning in Brazil. J. Geophys. Res. Atmos. 103, 32041–32050.
Moffet, R., Prather, K., 2009. In-situ measurements of the mixing state and optical properties of soot with implications for radiative forcing estimates. P. Natl. Acad. Sci. 106, 11872–11877.
Moteki, N., Kondo, Y., 2007. Effects of mixing state on black carbon measurements by laser-induced incandescence. Aerosol Sci. Technol. 41, 398–417.
Pósfai, M., Gelencsér, A., Simonics, R., Arató, K., Li, J., Hobbs, P.V., Buseck, P.R., 2004. Atmospheric tar balls: particles from biomass and biofuel burning. J. Geophys. Res. Atmos. 109, 06213.
Ram, K., Sarin, M.M., 2009. Absorption coefficient and site-specific mass absorption efficiency of elemental carbon in aerosols over urban, rural, and high-altitude sites in India. Environ. Sci. Technol. 43, 8233–8239.
Schnaiter, M., Linke, C., Möhler, O., Naumann, K.H., Saathoff, H., Wagner, R., Schurath, U., 2005. Absorption amplification of black carbon internally mixed with secondary organic aerosol. J. Geophys. Res. Atmos. 110, D19204.
Sorensen, C.M., 2001. Light scattering by fractal aggregates: a review. Aerosol Sci. Technol. 35, 648–687.
Srinivas, B., Sarin, M.M., 2013. Light absorbing organic aerosols (brown carbon) over the tropical Indian Ocean: impact of biomass burning emissions. Environ. Res. Lett. 8 https://doi.org/10.1088/1748-9326/8/4/044042.
Tan, Y., Wang, H., Shi, S., Shen, L., Zhang, C., Zhu, B., Guo, S., Wu, Z., Song, Z., Yin, Y., Liu, A., 2020. Annual variations of black carbon over the yangtze river delta from 2015 to 2018. J. Environ. Sci. 96, 72–84.
Teng, S., Liu, C., Schnaiter, M., Chakrabarty, R.K., Liu, F., 2019. Accounting for the effects of nonideal minor structures on the optical properties of black carbon aerosols. Atmos. Chem. Phys. 19, 2917–2931.
Utry, N., Ajtai, T., Filep, A., Pinter, M., Torok, Z., Bozoki, Z., Szabo, G., 2014. Correlations between absorption Angstrom exponent (AAE) of wintertime ambient urban aerosol and its physical and chemical properties. Atmos. Environ. 91, 52–59.
Wang, J., Nie, W., Cheng, Y., Shen, Y., Chi, X., Wang, J., Huang, X., Xie, Y., Sun, P., Xu, Z., Qi, X., Su, H., Ding, A., 2018a. Light absorption of brown carbon in eastern China based on 3-year multi-wavelength aerosol optical property observations and an improved absorption Ångström exponent segregation method. Atmos. Chem. Phys. 18, 9061–9074.
Wang, Y., Liu, F., He, C., Bi, L., Cheng, T., Wang, Z., Zhang, H., Zhang, X., Shi, Z., Li, W., 2017. Fractal dimensions and mixing structures of soot particles during atmospheric processing. Environ. Sci. Technol. Lett. 4, 487–493.
Wang, Y., Ma, P., Peng, J., Zhang, R., Jiang, J., Easter, R., Yung, Y., 2018b. Constraining aging processes of black carbon in the community atmosphere model using environmental chamber measurements. J. Adv. Model. Earth Syst. 10, 2514–2526.
Wu, Y., Cheng, T., Liu, D., Allan, J.D., Zheng, L., Chen, H., 2018. Light Absorption Enhancement of black carbon aerosol constrained by particle morphology. Environ. Sci. Technol. 52, 6912–6919.
Yang, M., Howell, S.G., Zhuang, J., Huebert, B.J., 2008. Attribution of aerosol light absorption to black carbon, brown carbon, and dust in China – interpretations of atmospheric measurements during EAST-AIRE. Atmos. Chem. Phys. 9, 2035–2050.
Yuan, Q., Xu, J., Liu, L., Zhang, A., Liu, Y., Zhang, J., Wan, X., Li, M., Qin, K., Cong, Z., Wang, Y., Kang, S., Shi, Z., Posfai, M., Li, W., 2020. Evidence for large amounts of brow carbonaceous tarballs in the himalayan atmosphere. Environ. Sci. Technol. Lett. https://doi.org/10.1021/acs.estlett.0c00735.
Yurkin, M.A., Hoekstra, A.G., 2007. The discrete dipole approximation: an overview and recent developments. J. Quant. Spectrosc. Radiat. Transfer 106, 558–589.
Yurkin, M.A., Hoekstra, A.G., 2011. The discrete-dipole approximation code ADDA: capabilities and known limitations. J. Quant. Spectrosc. Radiat. Transfer 112, 2234–2247.